ANALYSIS OF A DIESEL-ENGINE DRIVEN GENERATING UNIT AND THE POSSIBILITY FOR VOLTAGE FLICKER

P. M. Anderson, Fellow, IEEE
Power Math Associates, Inc.
San Diego, California

M. Mirheydar, Member, IEEE
Siemens Energy and Automation, Inc.
Empros Power Systems Control Division
Plymouth, Minnesota

Abstract

Key Words
Voltage variation, flicker, internal combustion engine, engine driven generator, cogenerator, methane-fueled generating plant, dynamic power system simulation.

Introduction

The regulations governing the utility industry encourage the attachment to the power system of various forms of non-utility generation. This paper describes a problem observed with a particular engine-driven generating unit that utilizes methane fuel, which is available from a former waste dumping site. The fuel is a limited resource, but the supply is sufficient to fuel a small generating unit, which is connected to the local distribution feeder. In the case under study, the distribution feeder is typical 12 kV circuit, and the generating unit is located some distance from the utility substation that is the normal source of supply for the feeder. A general view of the physical system is shown in Figure 1, with the utility equivalent on the right and the engine-driven generator on the left. Loads are distributed along the length of the feeder and are assumed to be balanced on the three phases.

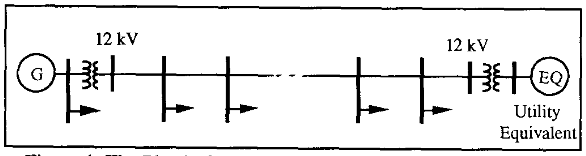

Figure 1 The Physical Arrangement of Distribution Feeder and Engine-Driven Generating Unit

The generating unit of this study was installed and operated for several months, providing a portion of the energy required to serve the load connected along the feeder. After a time, complaints of voltage flicker were received by the utility. The most frequent complaints were from a small business where the operators of electrically illuminated equipment were annoyed by the variation in light intensity. Subsequent investigation showed that large voltage variations were in evidence on the feeder, and were of greatest magnitude when the non-utility generating unit was in operation.

The complaints of flicker resulted in several system tests, performed by both the utility and the owner of the generating unit, to determine the exact nature of the voltage variation and its cause. A photographic scan of a typical voltage chart recorded by the utility during one of these test is shown in Figure 2, which shows a sudden increase in voltage variation at the instant the plant breaker is closed. The voltage trace is almost perfectly flat prior to the breaker closing. These charts showed random bursts of voltage oscillation, the cause of which was unknown. One theory of the cause reasoned that the bursts could be due to some light industrial motors on the feeder. Another theory blamed the voltage variation on the generator or its prime mover. Both of these theories were explored analytically, using a standard transient stability program, where the utility system, the feeder, all of the loads, and the non-utility generating unit were all represented. The utility system was represented as an infinite bus, but the feeder, all loads, and the engine driven generator were represented in detail.

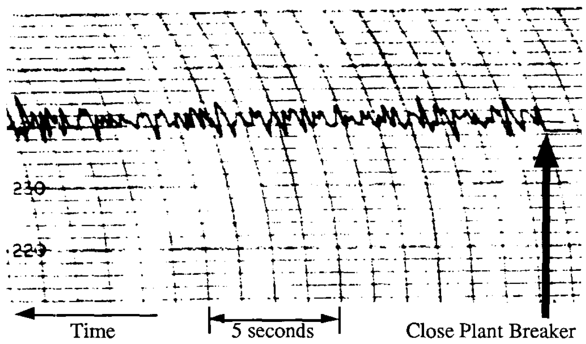

Figure 2 Voltage Variations Recorded on the Tested Feeder

Simulations showed that the type and magnitude of voltage variations were not due to load switching, as there were no loads large enough to cause the magnitude of variation observed. Closer inspection, however, revealed an interesting feature of the bursts of voltage variation, namely, each burst begins with a negative voltage excursion. This would be possible for a large motor starting, but positive excursions would be expected when switching the motor off. One way for all bursts to have an initial negative swing could be due to misfiring of the engine, and thereby causing a sudden decrease in torque. This theory proved to be the correct one, as the careful modeling of the engine performance, including misfires, made it possible to duplicate all of the bursts of voltage flicker.

Diesel Engine Operation

The operation of a four-cycle internal combustion engine driving a synchronous generator is evaluated in order to understand the possible source of frequencies observed on the utility distribution system. Some of the basic constants for shaft speeds of interest are shown in Table 1 and are described as follows.

94 SM 416-8 EC A paper recommended and approved by the IEEE Electric Machinery Committee of the IEEE Power Engineering Society for presentation at the IEEE/PES 1994 Summer Meeting, San Francisco, CA, July 24 - 28, 1994. Manuscript submitted August 2, 1993; made available for printing June 27, 1994.

n = Synchronous Speed of Shaft, rev / min
T_{REV} = Period of One Revolution of Shaft, s
$T_{PS} = 2T_{REV}$ = Period of Engine Power Stroke, s

$$f_{PS} = \frac{1}{T_{PS}} = \text{Frequency of Power Stroke, Hz} \tag{1}$$

From the table, it is noted that each cylinder experiences a power stroke at the frequency noted in the right-hand column. Frequencies between about 6 and 10 hertz are the most sensitive for human perception, with about 8.8 Hz being the most critical [1,3]. In this frequency range, a voltage deviation of 0.7 percent or more can be observed by most people. The most sensitive frequencies of those listed in Table 1 are the 7.5 Hz and 10.0 Hz entries.

Table 1 Basic Constants for Internal Combustion Engines

Number of Poles	n rev/min	T_{REV} s	T_{PS} s	f_{PS}
2	3600	0.01667	0.03333	30.00
4	1800	0.03333	0.06667	15.00
6	1200	0.05000	0.10000	10.00
8	900	0.06667	0.13333	7.50
10	720	0.08333	0.16667	6.00
12	600	0.10000	0.20000	5.00
14	514	0.11667	0.23333	4.28
16	450	0.13333	0.26667	3.75
18	400	0.15000	0.30000	3.33
20	360	0.16667	0.33333	3.00

If the engine has N_C cylinders, the number of cylinders firing in each revolution, N_F, of the shaft is given by

$$N_F = \frac{N_C}{2} \tag{2}$$

and the cylinders are arranged symmetrically on the crankshaft so that these N_F firings are equally spaced in angle. The angular separation between consecutive firings of a four-cycle engine is given by

$$\theta_C = \frac{720°}{N_C} \text{ degrees} \tag{3}$$

and the time between consecutive cylinder firings is given by

$$T_F = \frac{T_{REV}}{N_F} = \frac{T_{PS}}{N_C} \text{ s} \tag{4}$$

The firing time and angle are illustrated in Figure 3(a). This is not the firing sequence, but simply the angular displacement on the shaft between consecutive firing events. Figure 3(b) shows the familiar two-revolution sequence; intake, compression, power, and exhaust for a four-cycle engine, shown as I, C, P, E in the figure. The engine under study is a 900 rpm engine, with the attributes described in Table 1. The period of each revolution of this engine is 0.0667 seconds. The power stroke is the represented by the dark area and is of 0.033 seconds duration or one-half of one revolution. Power strokes occur every 0.1333 seconds, and this period corresponds to a frequency of 7.5 Hz.

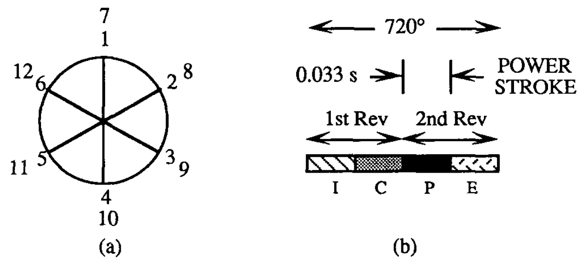

Figure 3 Basic Engine Firing Configuration

If all 12 cylinders are laid out graphically, the engine timing can be illustrated as shown in Figure 4. From this figure it is observed that, in the steady state, exactly three cylinders should always be firing simultaneously for a 12 cylinder engine. Moreover, the period of each firing, such as from a to b or b to c, is 0.011 seconds, representing a frequency of 90 Hz. A Fourier analysis of the engine torque should reveal a 90 Hz component. Should any one cylinder react differently from the others, such as a misfire, a 7.5 Hz component should be observed, and generally all multiples of 7.5 Hz in varying magnitudes.

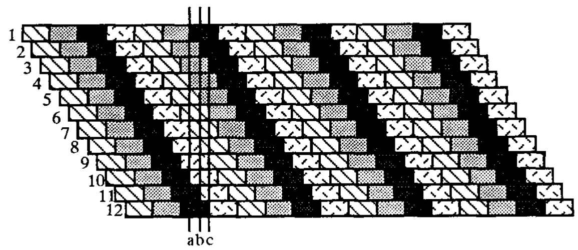

Figure 4 Timing of the 12 Cylinder Engine

The basic 7.5 Hz frequency of power pulses in this engine is cause for concern, since this is a frequency at which human perception of voltage flicker is approximately at its a maximum. This is illustrated in Figure 5, which shows the results of tests that recorded the percentages of observers that are expected to perceive voltage flicker at different frequencies [1]. Similar results are reported in other references [2,3].

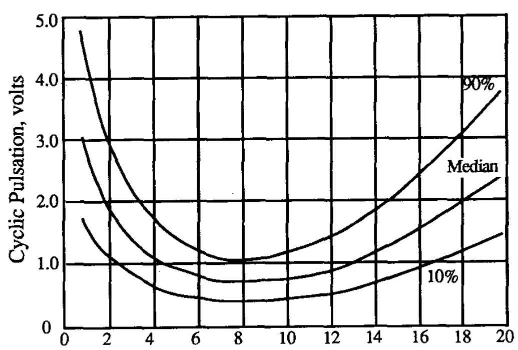

Figure 5 Cyclic Pulsations of Voltage of a 115 Volt Tungsten Filament Lamp at which Flicker is Perceptible [1]

Figure 5 shows that at least one-half of the observers can detect a flicker of 0.7 percent or more in the frequency range of 6 to 10 Hz. This suggests that 12 cylinder, engine-driven generators with synchronous speeds of 720, 900, or 1200 rev/min are the most likely to cause voltage variations in the critical range due to the frequency of ignition, as noted in Table 1. The 900 rev/min engine falls in the middle of this critical range.

Engine Torque Production

In order to perform analytical studies of the engine-driven generator, it is necessary to derive a model of the torque production of the prime mover. The development of engine torque for internal combustion engines is well known, and is discussed in textbooks on the subject. The book by Taylor [4] shows the resultant torque of one cylinder on the crankshaft, a normalized version of which is shown in Figure 6.

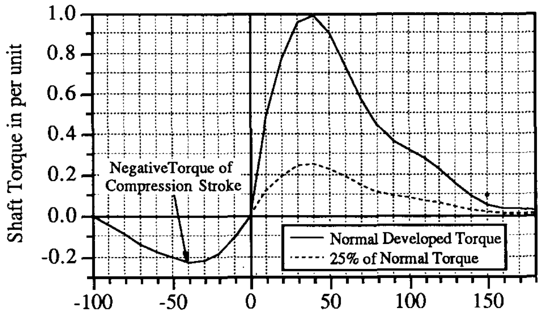

Figure 6 Developed Shaft Torque of Internal Combustion Engine

The torque curve in Figure 6 shows the negative torque required for the compression stroke, followed by the positive torque of the power stroke, normalized to the peak value of torque. Also shown in Figure 6, by the dashed line, is a curve representing 25% of the normal torque, which might be used for a cylinder that experiences partial firing due to ingestion of fuel with low calorie content. Several such partial firing studies, using varying percentages of full torque, were made as part of the study described here.

Figure 6 represents the torque produced by only one cylinder of the engine. To determine the total torque, the curve of Figure 4 may be digitized and replicated at 60° intervals, representing all 12 cylinders of the engine, and the total torque determined by summing the 12 components. The mean of this total is then computed and used as the base for averaging the total torque to a value of 1.0 per unit. This normalized torque shown in Figure 7, may be used in a transient stability program, entering the prime mover torque as a tabulation of torque values as a function of time. The pulsating nature of the engine torque is clearly evident in Figure 7 and the frequency of the pulsations is 90 Hz. This frequency is clearly shown in the fast Fourier transform of the torque, which is displayed in Figure 8. The torque is given in appendix Table A.1.

When one cylinder misfires, the torque for that cylinder is greatly reduced. The amount of the reduction can be a matter of speculation, as noted in the reduced torque curve in Figure 6. If we assume the net torque of the misfiring cylinder to be zero, the resulting torque curve is shown in Figure 9.

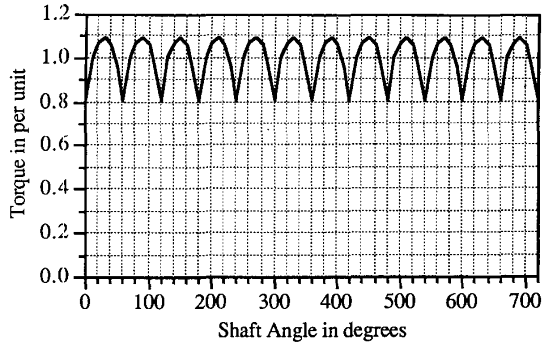

Figure 7 Normalized Engine Torque for Two Revolutions

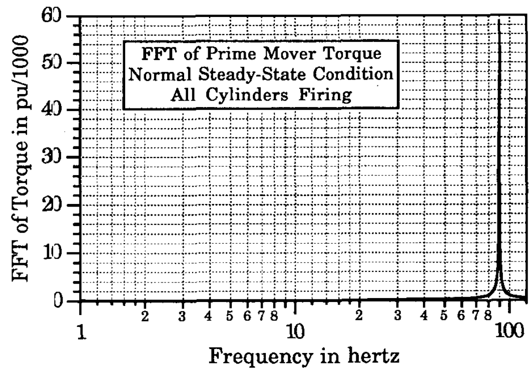

Figure 8 FFT of the Prime Mover Torque - Normal Conditions

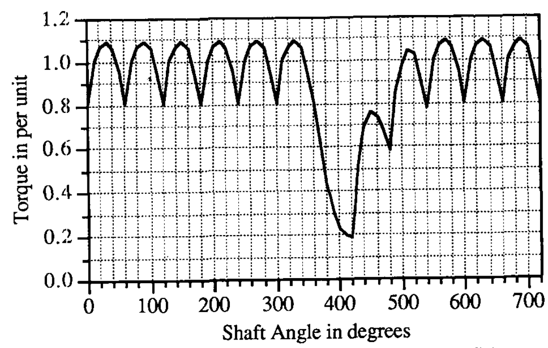

Figure 9 Engine Torque with Cylinder #7 Misfiring

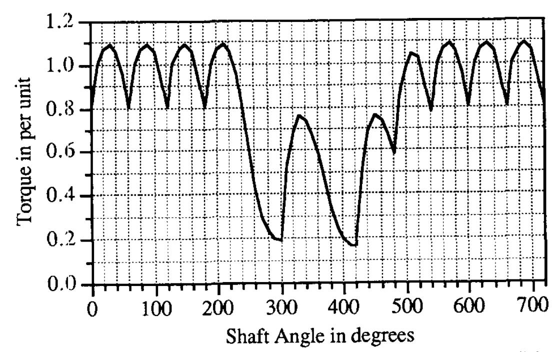

Figure 10 Engine Torque with Cylinders #5 and #7 Misfiring

Figure 10 shows the engine torque resulting from misfiring of alternate cylinders, which results in two negative pulses 120° apart.

If two adjacent cylinders misfire, the resulting torque production actually goes negative briefly, as shown in Figure 11. This is due to the negative torque still required for the compression strokes of the two misfiring cylinders, resulting in a very large torque disturbance.

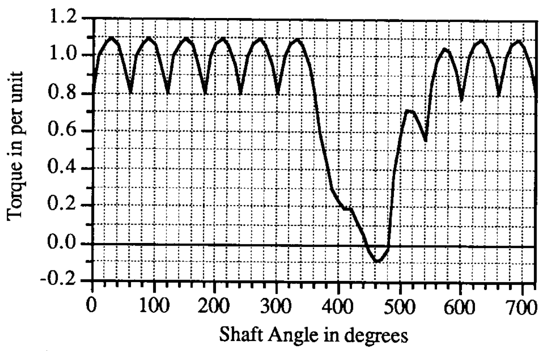

Figure 11 Engine Torque with Cylinders #7 and #8 Misfiring

All of the foregoing torque patterns are of interest. Should the engine receive a quantity of fuel of low calorie content, misfiring may occur on one or more cylinders. Stability simulations may be used to translate the torque disturbances into voltage variations on the connected system, which may then be compared to the observe voltage variations measured on the distribution feeder.

Simulated Results

Simulations were performed for various steady state conditions that represent the normal feeder loading at different times of the day and seasons of the year. The major point of interest is to determine the type of voltage variation that will be observed due to changes in the prime mover torque, described above.

It was observed from careful review of many field tests that the voltage variations often occurred in similar patterns. These patterns were given arbitrary names, Type A, B, etc., and the repetition of these patterns was noted on the recordings. Three of these patterns that were observed to occur regularly are shown in Figure 12. In these traces, time advances from left to right in the normal manner. Each of the traces shown is one second long. The vertical scale is two percent per major division. Peak-to-peak variations of three percent were found to be common and occasional bursts of higher amounts were observed on the charts. The frequencies of the observed oscillations were always in the range of 6 to 10 Hz, but the oscillations are not purely sinusoidal.

Working on the theory that either total or partial misfiring of one or more cylinders might lead to this type of behavior, a number of different torque patterns, similar to those of Figures 12 were tried. These torque models were used as the prime mover torque output to the generator in a stability simulation of the system shown in Figure 1. This occasionally required some adjustment to closely match the observed voltage patterns.

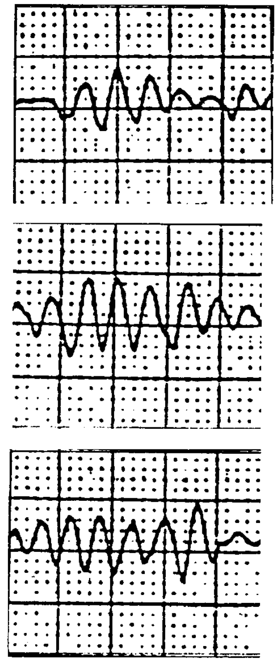

Figure 12 Disturbance Waveform Types from Field Tests

Disturbance Pattern C

Disturbance Pattern C is characterized by the following sequence:

- a step to a large peak-to-peak oscillation, then
- decreasing peak-to-peak oscillations, then
- a larger oscillation, then
- decaying oscillations to normal voltage.

The stability simulation of this pattern is shown in Figure 13.

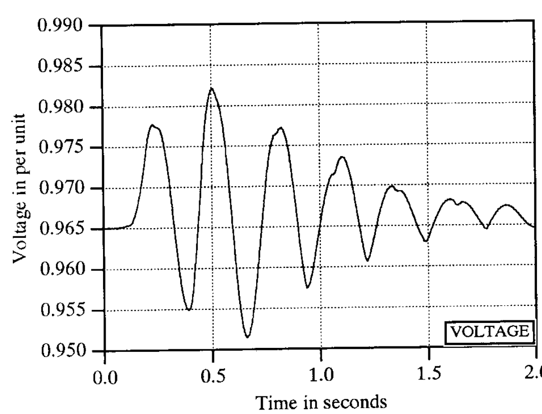

Figure 13 Computer Simulation of Bus Voltage for Pattern #1

The peak-to-peak maximum oscillation from the simulation is about 3.0 percent, which is roughly equal to several voltage variations observed on the power system. The prime mover torque used to generate this pattern is shown in Figure 14.

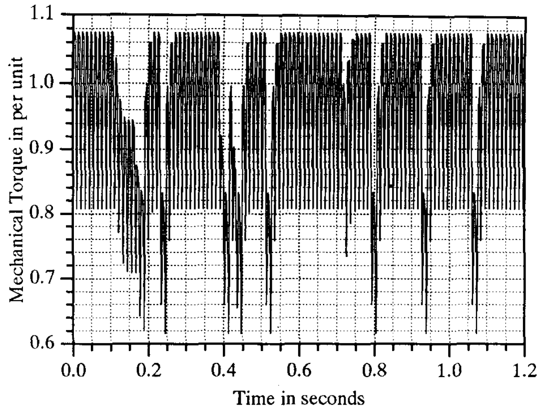

Figure 14 Prime Mover Torque for Pattern C

A Fast Fourier Transform of this prime mover torque is shown in Figure 15. As expected the predominate frequency is the 90 Hz component of the torque signal, which is due to the pulsating torque from the individual cylinders. With the regular pattern disturbed by the misfiring, however, new components of torque are in evidence. These new components are dominated by a 7.5 Hz component, with integral multiples of 7.5 Hz also present, but with diminishing magnitude. The 7.5 component is of considerable interest because of the sensitivity of the human eye to frequencies in this neighborhood.

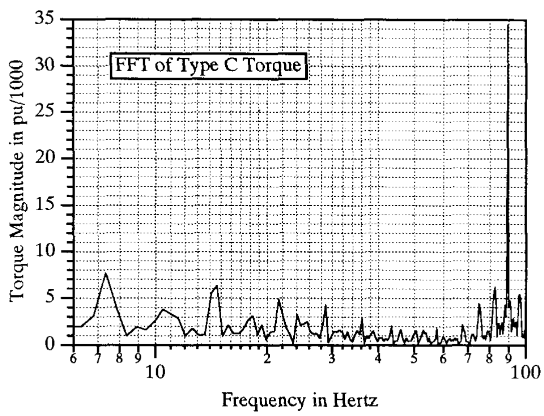

Figure 15 FFT of Pattern C Prime Mover Torque

Disturbance Pattern D

Disturbance Pattern D from Figure 12 is characterized by the following sequence:

- a step to a large peak-to-peak oscillations, then
- steadily decaying oscillations to normal voltage

The stability simulation of this pattern is shown in Figure 16.

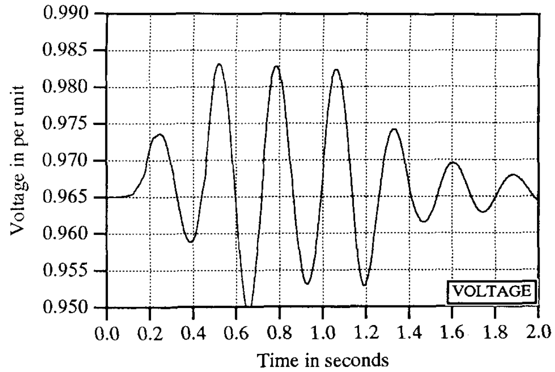

Figure 16 Computer Simulation of Bus Voltage for Pattern D

The peak-to-peak voltage swing for this pattern is 3.0 percent. The prime mover torque used to generate this pattern is shown in Figure 17 and the FFT of this torque pattern is shown in Figure 18. As before, the 7.5 Hz component is clearly evident.

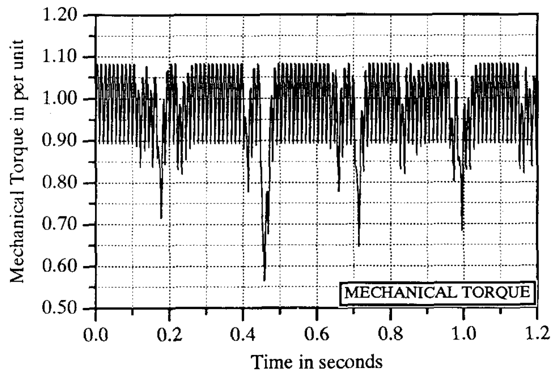

Figure 17 Prime Mover Torque for Pattern D

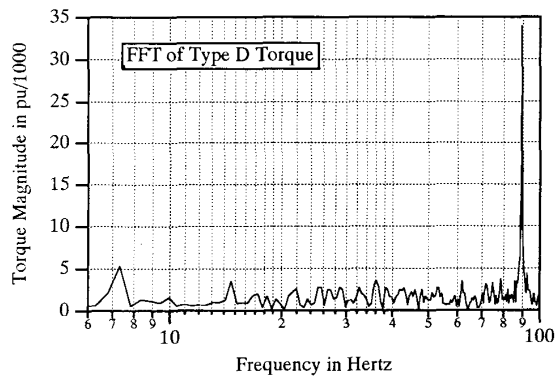

Figure 18 FFT of Pattern D Prime Mover Torque

Disturbance Pattern E

Disturbance Pattern E from Figure 12 is usually characterized in the field tests by the following sequence:

- growing oscillations for several cycles, then
- a smaller oscillation, then
- a much larger oscillation, then
- decaying oscillations to normal voltage

The stability simulation of this pattern is shown in Figure 19.

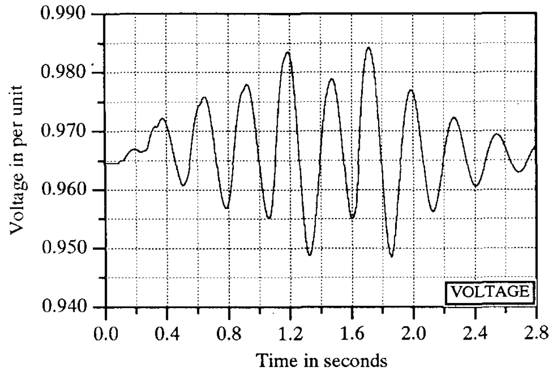

Figure 19 Computer Simulation of Bus Voltage for Pattern E

The maximum peak-to-peak voltage deviation for this pattern is about 3.5 percent. The prime mover torque used to generate this pattern is shown in Figure 20 and the FFT of this torque is shown in Figure 21. As before, the 7.5 Hz component is relatively strong.

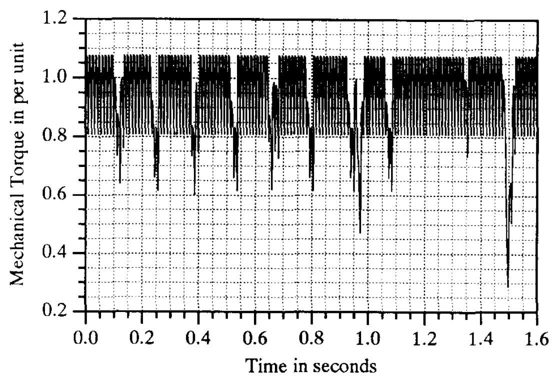

Figure 20 Prime Mover Torque for Pattern E

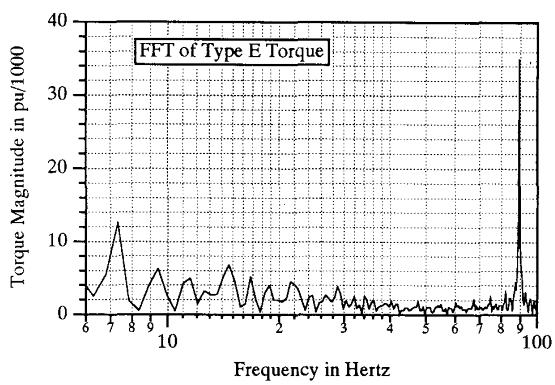

Figure 21 FFT of Pattern E Prime Mover Torque

Frequency Domain Analysis of the Voltage

Even though there is a prominent 7.5 Hz component in the prime mover torque, it is not clear that this frequency is observable on the generator terminal voltage. Figure 22 shows the FFT of terminal generator voltage for the case of Pattern C. This trace shows several frequencies, with the 7.5 Hz component clearly predominant. Since human perception is most responsive to the range between 6 and 10 Hz, this is the only frequency of concern in this voltage response, and its magnitude is adequate to likely result in flicker complaints.

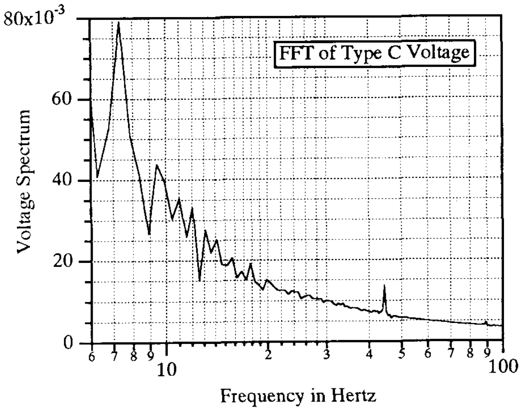

Figure 22 FFT of Pattern C Terminal Voltage

The reason that the 7.5 Hz oscillation is larger than the higher frequency components that are present in the mechanical torque signal is because of the filtering effect of the generator. Field tests of synchronous machines have verified that the generator acts as a low pass filter [5,6]. This causes the 7.5 Hz component to pass the generator at much higher magnitude than any of the higher frequency components that are present in the mechanical torque.

Conclusions

Flicker complaints have been received from customers connected to a distribution feeder and the voltage causing the flicker has been measured in field tests. These tests confirmed that the voltage vary by up to three percent from normal and this variation begins when the engine-driven generator breaker is closed. The reason for the variation is believed due to the poor quality of fuel used in a Diesel engine driven generator connected to the distribution feeder, where the low calorie fuel causes occasional misfiring of the engine. Misfiring of the engine can cause large changes in mechanical torque of the prime mover. This paper shows that such torque changes can cause voltage variations with frequency components that may cause lamp flicker. It should not be implied that engine-driven generators will cause voltage variations of the type noted here, since the variation of voltage depends on other factors, such as the strength of the interconnection to the utility system. The case under examination here is a rather weak interconnection, can this is partly to blame for the voltage behavior and the flicker complaints.

This paper also shows that the use of 900 rpm engine-driven generators might be candidates for causing voltage variations on a distribution feeder, due to the natural frequency spectrum of the engine. Utilities that expect to connect such an engine-driven generator might wish to examine the dynamics of the interconnection prior to its completion, using a stability program or similar type of simulation. For the case under study, the simulations of the system proved to be an effective way of showing that the poor engine fuel quality is capable of causing the type of disturbance observed in the field tests, thereby producing voltage waveforms that might cause lamp flicker under certain system conditions.

In testing the system under study, the authors tried many possible remedial solutions, including adding a flywheel to the prime mover, adding a very fast excitation system, improving the response of the speed governor, and adding a static var system. None of these solutions were adequate to overcome the relatively large magnitude of the mechanical torque disturbances. Had these simulations been performed prior to the installation of the generating unit, a considerable saving could have been realized to both the generator owner and the utility.

There are undoubtedly many 900 rpm engine-driven generators in service on utility systems. There are also an increasing number of small generating units being added that use fuel of possibly low calorie content, and that may be connected to the system at remote or weak locations. These combinations present a high likelihood for voltage flicker that may be objectionable to nearby utility customers.

Stability simulation provides a convenient method for evaluating voltage variation under the conditions described. The amount of voltage variation depends on the strength of the utility supply system at the point of interconnection as well as to the misfiring of the engine. One way to evaluate the possiblity of flicker problems is by worst case analysis. The engineer can perform simulations for the condition identified here as Pattern E, for which the mechanical torque values are provided in Table A.2 of the Appendix 2. This is one of the worst cases found for the system under study. Using these mechanical torque values, a study can be performed for any system, using the power system parameters at the point of generating unit interconnection. If the utility system is very strong, the computed voltage variations will be small. However, for a relatively weak system, the variations may be large enough to suggest finding an alternate solution. The alternatives might include finding another location for the engine-driven generator, specifying a different engine prime mover, or planning for reinforcements of the utility system at the point of interconnection.

References

1. Sauter, D. M., "Voltage Fluctuations on Power System," Chapter 9 of **Distribution Systems**, published by Westinghouse Electric Corporation, 1965.

2. Mirra, C., Ed., **Connection of Flutuating Loads**, a report prepared by the Working Group on Disturbances, International Union for Electroheat, Paris, July, 1988.

3. Working Group on Disturbances, **Flicker Measurement and Evaluation**, Second Revised Edition, International Union for Electroheat, Paris, 1992.

4. Taylor, Charles Fayette, **The Internal-Combustion Engine in Theory and Practice, Vol. II: Combustion, Fuels, Materials, Design**, The MIT Press, Cambridge, MA, 1968.

5. Anderson, P.M., B. L. Agrawal, and J. E. Van Ness, **Subsynchronous Resonance in Power Systems**, IEEE Press, Piscataway, NJ, 1990.

6. Ontario Hydro Engineers, "Determination of Synchronous Machine Stability Study Constants," EPRI Report EL-1424, v. 2, EPRI Project 997-2, December 1980.

Biographies of the Authors

P. M. Anderson was born in Iowa and holds the B.S., M.S., and Ph.D. degrees in Electrical Engineering from Iowa State University. He has worked for a utility, taught E.E. at Iowa State and Arizona State Universities, and served as an EPRI research manager. He is currently Principal Engineer at Power Math Associates, a consulting engineering firm in San Diego, California.

Mahmood Mirheydar was born in Iran. He obtained the B.S. and M.S. degrees from the University of Iowa and the Ph.D. degree from Iowa State University, all in Electrical Engineering. He worked as a consulting engineer for several years, specializing in power system dynamic analysis. He is currently Senior Software Engineer with Empros Power Systems, a division of Siemens Energy and Automation, Inc. located in Plymouth, Minnesota.

Appendix 1

Table A.1 provides the normalized torque values for the 900 rpm engine, operating under normal conditions.

Table A.1 Normalized Torque for Normal Operating Conditions

Angle, degrees	Time, seconds	Normalized
0	0.00000	0.807067822
20	0.00373	1.074781573
40	0.00746	1.065923534
60	0.01119	0.807067822
80	0.01492	1.074781573
100	0.01865	1.065923534
120	0.02238	0.807067822
140	0.02611	1.074781573
160	0.02984	1.065923534
180	0.03357	0.807067822
200	0.03730	1.074781573
220	0.04103	1.065923534
240	0.04476	0.807067822
260	0.04849	1.074781573
280	0.05222	1.065923534
300	0.05595	0.807067822
320	0.05968	1.074781573
340	0.06341	1.065923534
360	0.06714	0.807067822
380	0.07087	1.074781573
400	0.07460	1.065923534
420	0.07833	0.807067822
440	0.08206	1.074781573
460	0.08579	1.065923534
480	0.08952	0.807067822
500	0.09325	1.074781573
520	0.09698	1.065923534
540	0.10071	0.807067822
560	0.10444	1.074781573
580	0.10817	1.065923534
600	0.11190	0.807067822
620	0.11563	1.074781573
640	0.11936	1.065923534
660	0.12309	0.807067822
680	0.12682	1.074781573
700	0.13055	1.065923534
720	0.13428	0.807067822

Appendix 2

Table A.2, which is given in four parts, provides the normalized mechanical torque values for the 900 rpm engine operating under the conditions described in this paper as Case E.

Table A.2 Normalized Mechanical Torque for Case E, Part 1

Angle, deg	Time, s	Torque, pu	Angle, deg	Time, s	Torque, pu
0	0.00000	0.80707	1020	0.19023	0.76030
20	0.00373	1.07478	1040	0.19396	1.05664
40	0.00746	1.06592	1060	0.19769	1.05930
60	0.01119	0.80707	1080	0.20142	0.80167
80	0.01492	0.99781	1100	0.20515	1.07478
100	0.01865	0.96691	1120	0.20888	1.06592
120	0.02238	0.73327	1140	0.21261	0.80707
140	0.02611	1.03057	1160	0.21634	1.07478
160	0.02984	1.03393	1180	0.22007	1.06592
180	0.03357	0.78503	1200	0.22380	0.80707
200	0.03730	1.06571	1220	0.22753	1.07478
220	0.04103	1.06261	1240	0.23126	1.06592
240	0.04476	0.80437	1260	0.23499	0.80707
260	0.04849	1.07478	1280	0.23872	1.07478
280	0.05222	1.06592	1300	0.24245	1.06592
300	0.05595	0.80707	1320	0.24618	0.80707
320	0.05968	1.07478	1340	0.24991	1.02090
340	0.06341	1.06592	1360	0.25364	0.99661
360	0.06714	0.80707	1380	0.25737	0.75541
380	0.07087	1.07478	1400	0.26110	1.04383
400	0.07460	1.06592	1420	0.26483	1.04353
420	0.07833	0.80707	1440	0.26856	0.79164
440	0.08206	1.07478	1460	0.27229	1.06843
460	0.08579	1.06592	1480	0.27602	1.06360
480	0.08952	0.80707	1500	0.27975	0.80518
500	0.09325	1.07478	1520	0.28348	1.07478
520	0.09698	1.06592	1540	0.28721	1.06592
540	0.10071	0.80707	1560	0.29094	0.80707
560	0.10444	1.07478	1580	0.29467	1.07478
580	0.10817	1.06592	1600	0.29840	1.06592
600	0.11190	0.80707	1620	0.30213	0.77017
620	0.11563	1.07478	1640	0.30586	1.05267
640	0.11936	1.06592	1660	0.30959	1.04993
660	0.12309	0.80707	1680	0.31332	0.79605
680	0.12682	0.99781	1700	0.31705	1.07025
700	0.13055	0.96691	1720	0.32078	1.06592
720	0.13428	0.73327	1740	0.32451	0.80707
740	0.13801	1.03057	1760	0.32824	1.07478
760	0.14174	1.03393	1780	0.33197	1.06592
780	0.14547	0.78503	1800	0.33570	0.80707
800	0.14920	1.06571	1820	0.33943	1.07478
820	0.15293	1.06261	1840	0.34316	1.06592
840	0.15666	0.80437	1860	0.34689	0.80707
860	0.16039	0.99781	1880	0.35062	1.07478
880	0.16412	0.96691	1900	0.35435	1.06592
900	0.16785	0.73327	1920	0.35808	0.80707
920	0.17158	0.87663	1940	0.36181	1.07478
940	0.17531	0.83590	1960	0.36554	1.06592
960	0.17904	0.63743	1980	0.36927	0.80707
980	0.18277	0.97728	2000	0.37300	1.07478
1000	0.18650	0.99863			

Table A.2 Normalized Mechanical Torque for Case E, Part 2

Angle, deg	Time, s	Torque, pu	Angle, deg	Time, s	Torque, pu
2020	0.37673	1.06592	3020	0.56323	1.07478
2040	0.38046	0.80707	3040	0.56696	1.06592
2060	0.38419	1.07478	3060	0.57069	0.80707
2080	0.38792	1.06592	3080	0.57442	1.07478
2100	0.39165	0.80707	3100	0.57815	1.06592
2120	0.39538	0.99781	3120	0.58188	0.80707
2140	0.39911	0.96691	3140	0.58561	1.07478
2160	0.40284	0.73327	3160	0.58934	1.06592
2180	0.40657	1.03057	3180	0.59307	0.80707
2200	0.41030	1.03393	3200	0.59680	1.07478
2220	0.41403	0.78503	3220	0.60053	1.06592
2240	0.41776	1.06571	3240	0.60426	0.80707
2260	0.42149	1.06261	3260	0.60799	1.07478
2280	0.42522	0.80437	3280	0.61172	1.06592
2300	0.42895	0.99781	3300	0.61545	0.80707
2320	0.43268	0.96691	3320	0.61918	1.07478
2340	0.43641	0.73327	3340	0.62291	1.06592
2360	0.44014	0.83815	3360	0.62664	0.80707
2380	0.44387	0.78639	3380	0.63037	1.07478
2400	0.44760	0.60053	3400	0.63410	1.06592
2420	0.45133	0.95517	3420	0.63783	0.80707
2440	0.45506	0.98264	3440	0.64156	1.07478
2460	0.45879	0.74929	3460	0.64529	1.06592
2480	0.46252	1.05210	3480	0.64902	0.80707
2500	0.46625	1.05764	3500	0.65275	1.07478
2520	0.46998	0.80032	3520	0.65648	1.06592
2540	0.47371	1.07478	3540	0.66021	0.80707
2560	0.47744	1.06592	3560	0.66394	1.07478
2580	0.48117	0.80707	3580	0.66767	1.06592
2600	0.48490	1.07478	3600	0.67140	0.80707
2620	0.48863	1.06592	3620	0.67513	1.07478
2640	0.49236	0.80707	3640	0.67886	1.06592
2660	0.49609	1.07478	3660	0.68259	0.80707
2680	0.49982	1.06592	3680	0.68632	0.99781
2700	0.50355	0.77017	3700	0.69005	0.96691
2720	0.50728	1.05267	3720	0.69378	0.73327
2740	0.51101	1.04993	3740	0.69751	1.03057
2760	0.51474	0.79605	3760	0.70124	1.03393
2780	0.51847	1.07025	3780	0.70497	0.78503
2800	0.52220	1.06592	3800	0.70870	0.87329
2820	0.52593	0.80707	3820	0.71243	0.81507
2840	0.52966	1.07478	3840	0.71616	0.61986
2860	0.53339	1.06592	3860	0.71989	0.96424
2880	0.53712	0.80707	3880	0.72362	0.98595
2900	0.54085	1.07478	3900	0.72735	0.75198
2920	0.54458	1.06592	3920	0.73108	0.97513
2940	0.54831	0.80707	3940	0.73481	0.95862
2960	0.55204	1.07478	3960	0.73854	0.72652
2980	0.55577	1.06592	3980	0.74227	1.03057
3000	0.55950	0.80707	4000	0.74600	1.03393

Table A.2 Normalized Mechanical Torque for Case E, Part 3

Angle, deg	Time, s	Torque, pu	Angle, deg	Time, s	Torque, pu
4020	0.74973	0.78503	5020	0.93623	1.06592
4040	0.75346	1.06571	5040	0.93996	0.80707
4060	0.75719	1.06261	5060	0.94369	1.07478
4080	0.76092	0.80437	5080	0.94742	1.06592
4100	0.76465	1.07478	5100	0.95115	0.80707
4120	0.76838	1.06592	5120	0.95488	1.07478
4140	0.77211	0.80707	5140	0.95861	1.06592
4160	0.77584	1.07478	5160	0.96234	0.80707
4180	0.77957	1.06592	5180	0.96607	0.92085
4200	0.78330	0.80707	5200	0.96980	0.86789
4220	0.78703	1.07478	5220	0.97353	0.65946
4240	0.79076	1.06592	5240	0.97726	0.83241
4260	0.79449	0.80707	5260	0.98099	0.80391
4280	0.79822	1.07478	5280	0.98472	0.61540
4300	0.80195	1.06592	5300	0.98845	0.96821
4320	0.80568	0.80707	5320	0.99218	0.99532
4340	0.80941	1.07478	5340	0.99591	0.75760
4360	0.81314	1.06592	5360	0.99964	0.71028
4380	0.81687	0.80707	5380	1.00337	0.61372
4400	0.82060	1.07478	5400	1.00710	0.46956
4420	0.82433	1.06592	5420	1.01083	0.87581
4440	0.82806	0.80707	5440	1.01456	0.92197
4460	0.83179	1.07478	5460	1.01829	0.70792
4480	0.83552	1.06592	5480	1.02202	1.03396
4500	0.83925	0.80707	5500	1.02575	1.05102
4520	0.84298	1.07478	5520	1.02948	0.79493
4540	0.84671	1.06592	5540	1.03321	1.07478
4560	0.85044	0.77017	5560	1.03694	1.06592
4580	0.85417	1.05267	5580	1.04067	0.80707
4600	0.85790	1.04993	5600	1.04440	1.07478
4620	0.86163	0.79605	5620	1.04813	1.06592
4640	0.86536	1.07025	5640	1.05186	0.80707
4660	0.86909	1.06592	5660	1.05559	1.07478
4680	0.87282	0.80707	5680	1.05932	1.06592
4700	0.87655	1.07478	5700	1.06305	0.80707
4720	0.88028	1.06592	5720	1.06678	1.07478
4740	0.88401	0.80707	5740	1.07051	1.06592
4760	0.88774	1.07478	5760	1.07424	0.80707
4780	0.89147	1.06592	5780	1.07797	1.07478
4800	0.89520	0.80707	5800	1.08170	1.06592
4820	0.89893	1.07478	5820	1.08543	0.80707
4840	0.90266	1.06592	5840	1.08916	1.07478
4860	0.90639	0.80707	5860	1.09289	1.06592
4880	0.91012	1.07478	5880	1.09662	0.80707
4900	0.91385	1.06592	5900	1.10035	1.07478
4920	0.91758	0.80707	5920	1.10408	1.06592
4940	0.92131	1.07478	5940	1.10781	0.80707
4960	0.92504	1.06592	5960	1.11154	1.07478
4980	0.92877	0.80707	5980	1.11527	1.06592
5000	0.93250	1.07478	6000	1.11900	0.80707

Table A.2 Normalized Mechanical Torque for Case E, Part 4

Angle, deg	Time, s	Torque, pu	Angle, deg	Time, s	Torque, pu
6020	1.12273	1.07478	7020	1.30923	0.78503
6040	1.12646	1.06592	7040	1.31296	1.06571
6060	1.13019	0.80707	7060	1.31669	1.06261
6080	1.13392	1.07478	7080	1.32042	0.80437
6100	1.13765	1.06592	7100	1.32415	1.07478
6120	1.14138	0.80707	7120	1.32788	1.06592
6140	1.14511	1.07478	7140	1.33161	0.80707
6160	1.14884	1.06592	7160	1.33534	1.07478
6180	1.15257	0.80707	7180	1.33907	1.06592
6200	1.15630	1.07478	7200	1.34280	0.80707
6220	1.16003	1.06592	7220	1.34653	1.07478
6240	1.16376	0.80707	7240	1.35026	1.06592
6260	1.16749	1.07478	7260	1.35399	0.80707
6280	1.17122	1.06592	7280	1.35772	1.07478
6300	1.17495	0.80707	7300	1.36145	1.06592
6320	1.17868	1.07478	7320	1.36518	0.80707
6340	1.18241	1.06592	7340	1.36891	1.07478
6360	1.18614	0.80707	7360	1.37264	1.06592
6380	1.18987	1.07478	7380	1.37637	0.80707
6400	1.19360	1.06592	7400	1.38010	1.07478
6420	1.19733	0.77017	7420	1.38383	1.06592
6440	1.20106	1.05267	7440	1.38756	0.80707
6460	1.20479	1.04993	7460	1.39129	1.07478
6480	1.20852	0.79605	7480	1.39502	1.06592
6500	1.21225	1.07025	7500	1.39875	0.80707
6520	1.21598	1.06592	7520	1.40248	1.07478
6540	1.21971	0.80707	7540	1.40621	1.06592
6560	1.22344	1.07478	7560	1.40994	0.80707
6580	1.22717	1.06592	7580	1.41367	1.07478
6600	1.23090	0.80707	7600	1.41740	1.06592
6620	1.23463	1.07478	7620	1.42113	0.80707
6640	1.23836	1.06592	7640	1.42486	1.07478
6660	1.24209	0.80707	7660	1.42859	1.06592
6680	1.24582	1.07478	7680	1.43232	0.80707
6700	1.24955	1.06592	7700	1.43605	1.07478
6720	1.25328	0.80707	7720	1.43978	1.06592
6740	1.25701	1.07478	7740	1.44351	0.80707
6760	1.26074	1.06592	7760	1.44724	1.07478
6780	1.26447	0.80707	7780	1.45097	1.06592
6800	1.26820	1.07478	7800	1.45470	0.80707
6820	1.27193	1.06592	7820	1.45843	1.07478
6840	1.27566	0.80707	7840	1.46216	1.06592
6860	1.27939	1.07478	7860	1.46589	0.80707
6880	1.28312	1.06592	7880	1.46962	1.07478
6900	1.28685	0.80707	7900	1.47335	1.06592
6920	1.29058	0.99781	7920	1.47708	0.80707
6940	1.29431	0.96691	7940	1.48081	1.07478
6960	1.29804	0.73327	7960	1.48454	1.06592
6980	1.30177	1.03057	7980	1.48827	0.80707
7000	1.30550	1.03393	8000	1.49200	1.03630

DISCUSSION

DAVID D. ROBB, D. D. Robb and Associates, P.A., Consulting Engineers, Salina, Kansas: The authors report a skillfully conducted investigation of an important problem. The paper is a valuable contribution. Other engineers are likely to encounter similar problems to which the effective analytical procedures presented in this paper can be adapted.

The authors found that increased inertia and increased excitation system speed were not sufficient to overcome the effects of the mechanical torque disturbances. Did either remedy produce a significant reduction in the magnitude of the voltage fluctuations?

The authors refer in several places to the unfortunate generator speed of 900 rpm, that speed proving to be near-critical in the case of the four-cycle, 12-cylinder engine they investigated. The discusser suggests that 900 rpm is not a uniquely troublesome speed and that the troublesome speed will vary with the number of engine cylinders and with the competing engine designs of two and four cycles.

Manuscript received August 8, 1994.

P. M. Anderson and M. Mirheydar:

The authors appreciate the thoughtful comments of Dr. Robb and will attempt to respond by presenting additional information that was not included in the paper. First of all, some additional equations that describe an engine-driven generating unit are needed to properly respond to the questions raised. It is noted in the paper that the engine-generator shaft speed is given by

$$n = \frac{2f}{p} \quad \text{rev/s} \tag{a}$$

where

p = number of generator poles
f = system frequency

The shaft speed is 15 revolutions per second for the generator under study. Then the period of one revolution is

$$T_{REV} = \frac{1}{n} = \frac{p}{2f} \quad \text{s} \tag{b}$$

This time is 0.06667 seconds for the 60 Hz engine-generator under study.

The time between successive power strokes of a given cylinder is a function of the type of engine. For this parameter, we can write

$$T_{PS} = \frac{k_c T_{REV}}{2} \quad \text{s} \tag{c}$$

where

$$k_C = \begin{cases} 2 & \text{2 cycle engine} \\ 4 & \text{4 cycle engine} \end{cases} \tag{d}$$

Then (b) can be written as

$$T_{PS} = \frac{k_C p}{4f} \quad \text{s} \tag{e}$$

The engine under study in the paper is a 4 cycle engine and the generator is an 8 pole machine, so this time constant is computed to be 0.13333 seconds. This corresponds to the time between successive dark areas for any cylinder in Figure 4.

The frequency of power strokes for a given cylinder of the engine is given by the inverse of (e), or

$$f_{PS} = \frac{4f}{k_C p} \quad \text{Hz} \tag{f}$$

This frequency is computed to be 7.5 Hz for the engine under study.

The number of power strokes or firings per revolution is a function of the engine cycle type as well as the number of cylinders. This parameter can be computed as

$$N_F = \frac{2N_C}{k_C} \quad \text{power stokes per revolution} \tag{g}$$

This parameter is computed to be 6.0 for the engine under study.

The time between successive consecutive firing of cylinders in the engine is given as

$$T_F = \frac{T_{REV}}{N_F} = \frac{k_C p}{4fN_C} \quad \text{s} \tag{h}$$

which is 0.011111 seconds for the engine under study. This corresponds to the time measured from *a* to *b* or from *b* to *c* in Figure 4.

The frequency of occurrence of individual cylinder firings is given by the inverse of (h) or

$$f_F = \frac{4fN_C}{k_C p} \quad \text{Hz} \tag{i}$$

This frequency is noted in the paper to be 90 Hz for the engine under study.

We can also compute the duration of power strokes for each individual cylinder. This parameter is given as

$$T_P = \frac{T_{PS}}{k_C} \quad \text{s} \tag{j}$$

which is 0.03333 seconds for the engine under study. This corresponds to the length (time duration) of the dark areas for each cylinder in Figure 4.

Using the foregoing parameters, we can compute the number of overlapping power stokes for any engine. This parameter is defined as

$$k_{OL} = \frac{T_P}{T_F} = \frac{N_C}{k_C} \tag{k}$$

For the engine under study, this parameter is exactly 3.0, as noted in Figure 4 of the paper.

Mark's Handbook [7] gives a summary of several stationary and locomotive Diesel engines, some of which would be suitable for service as the prime mover for a 60 Hz generator of proper design. Table 2 summarizes some of these engines.

The authors hope that the foregoing discussion provides an adequate description for the case where engines of different designs might be used as prime movers for generators.

Dr. Robb also asked about the relative success achieved in attempting other means of mitigating the flicker, such as increased shaft inertia, faster excitation system, and more responsive speed governing. None of these remedial schemes were found to be adequate for reducing the disturbances to acceptable levels. The reason for this is that the torque disturbances are quite large in some cases, amounting to a significant fraction of the total prime mover output. These remedial schemes were found to be of little value in solving the observed problems.

The authors also tried to stabilize the simulated feeder voltage using high speed static var controllers, but these also proved to be inadequate. The SVC can be designed to hold the voltage nearly constant at the point of application, but the voltages on either side of the SVC were found to vary widely in response to the relatively large changes in line current caused by the engine torque changes.

It was the author's conclusion that improving the quality of fuel is probably the most effective method of solving the flicker problem for the engine under study and is a solution that can be achieved without extensive capital expenditure. However, this does involve an increased cost of fuel that may be unacceptable in some cases.

References

7. Marks, Lionel S., **Mechanical Engineers' Handbook**, 5th Edition, McGraw-Hill Book Company, New York, 1951.

Table 2 Summary of Typical Diesel Engines for Use as Generator Prime Movers

Manufacturer	N_C	n rev/min	n rev/s	T_{REV} s	p	k_C	T_{PS} s	f_{PS} Hz	N_F	T_F s	f_F Hz	θ_C	T_P s	k_{OL}
Baldwin	8	360.00	6.000	0.1667	20	4	0.3333	3.00	4.00	0.0417	24.000	90.00	0.083	2.000
Worthington	8	360.00	6.000	0.1667	20	4	0.3333	3.00	4.00	0.0417	24.000	90.00	0.083	2.000
Buckeye	8	400.00	6.667	0.1500	18	4	0.3000	3.33	4.00	0.0375	26.667	90.00	0.075	2.000
Copper-Bessemer	4	514.29	8.571	0.1167	14	4	0.2333	4.29	2.00	0.0584	17.133	180.00	0.058	1.000
Worthington	8	600.00	10.000	0.1000	12	4	0.2000	5.00	4.00	0.0250	40.000	90.00	0.050	2.000
Buckeye	3	600.00	10.000	0.1000	12	4	0.2000	5.00	1.50	0.0667	15.000	240.00	0.050	0.750
Nordberg	7	720.00	12.000	0.0833	10	4	0.1667	6.00	3.50	0.0238	42.000	102.86	0.042	1.750
Atlas-Imperial	4	900.00	15.000	0.0667	8	4	0.1333	7.50	2.00	0.0333	30.000	180.00	0.033	1.000
Study Generator	12	900.00	15.000	0.0667	8	4	0.1333	7.50	6.00	0.0111	90.000	60.00	0.033	3.000
Budd	6	1200.00	20.000	0.0500	6	4	0.1000	10.00	3.00	0.0167	60.000	120.000	0.025	1.500
Fairbanks-Morse	5	514.29	8.571	0.1167	14	2	0.1167	8.57	5.00	0.0233	42.833	144.00	0.058	2.500
Fairbanks-Morse	10	720.00	12.000	0.0833	10	2	0.0833	12.00	10.00	0.0083	120.00	72.00	0.042	5.000
General Motors	24	1800.00	30.000	0.0333	4	2	0.0333	30.00	24.00	0.0014	720.00	30.00	0.017	12.000

Manuscript received October 26, 1994.